ISSN: 2096-3246
Volume 54, Issue 06, August, 2022

CFD Simulations and Experimental Observation for Air-Water Two-phase Flow in a Vertical Pipe

Raid A. Mahmood[1,2*], Khalid Saleh[1], Veyan A. Musa[2], Enass Massoud[3], Saddam H. Al-Lwayzy[1], Ahmed Khalid Ibrahim[4], Ali Ghazi Mohammed[4], Lokman A. Abdulkareem[2,5]

School of Mechanical and Electrical Engineering, University of Southern Queensland,Toowoomba Australia[1]
Department of Mechanical Engineering, University of Zakho, Zakho, Iraq[2]
Mechanical Engineering Department, Arab Academy for Science, Technology and Cairo, Egyp[3]
Department of Mechanical Engineering, University of Mosul, Mosul, Iraq[4]
Institute of Fluid Dynamics, Helmholtz-Zentrum Dresden-Rossendorf, Germany[5]

Corresponding author: 1,2*

Keywords:
CFD, Pressure drops, Flow in vertical pipe, Wire mesh sensor.

ABSTRACT

Air-water two-phase flow development in a vertical pipe has been investigated through service of experiments and simulations in this research. Differential Pressure Transducers (DPTs) and Wire Mesh sensors (WMSs) are used to monitor the two-phase flow in a vertical pipe of 67 mm inlet diameter and 7000 mm length. Computational Fluid Dynamic (CFD) is used to evaluate the experiments of the air-water flow in the vertical pipe using a volume of fluid (VOF) model. The operating conditions cover a range of inlet air superficial velocities from 0.05 to 5 m/s. The inlet water superficial velocity remains constant at 0.2m/s and 0.4 m/s for all experiments. The results show that the bubbly flow is noted at low superficial velocities of gas, slug flow is observed at the moderate flow rates of gas, while the churn flow pattern is observed at high rates of gas. There is no significant effect when the Usl changed from 0.2 m/s to 0.4 m/s on the vertical flow lines. Pressure drop is recorded and compared with the CFD simulations. The CFD results are over estimation compared with the experimental pressured drop with maximum absolute error of 21% at Usl of 0.2 m/s and 25% at Usl 0.4 m/s.

1. INTRODUCTION

Air-water two-phase flow has received much attention as it has been applied in many applications in industry. Two-phase air-water is involved in various processes including pipeline networks [1]. In industry especially pipeline network applications, the two-phase flow patterns play a important role in pressure drop, flow development and pump selection [2]. In the industrial applications that involve two flow, the prediction of the governing correlations appropriate, the flow pattern regimes and the hydrodynamic characteristics of two-phase flow are crucial steps for accurate operation, simulation, modelling and optimization of that system [3]. Thus, the identification of flow structure, flow development and flow

characteristics can be achieved by flow patterns and pressure drop [4]. These parameters are essential to design an efficient pumping system [5]. Many studies have considered air-water two-phase flow development and its pressure drop because it influences the flow patterns, and it also reduces flow energy [6- 10]. So, two-phase flow patterns influence the pressure drop in pumping system.

Pressure drop has a significant role in vertical pipeline system and it was considered by many studies such as [7] who reported a correlation to predict the pressure drop for a two-phase flow in a vertical pipe, and [11] investigated the pressure drop for the two-phase flow using the gas/non-newtonian liquid system. [11] utilized a multiple-layer perceptron neural network (MLPNN) model to predict the pressure drop. The results revealed that the predicted pressure drop did not exceed 5%, a result that compared favorably with the experiments. [12] developed a transient non-isothermal gas-liquid two-phase flow model in the vertical pipeline. The authors validated the model with measured experimental data and field data. The model was used to investigate the influence of interfacial mass transfer of slip-rising bubbles on a two-phase flow of gas-liquid properties analysis. According to the simulation results, there was a slow mass transfer rate between oil dispersion and invasion gas was, so the gas was not immediately dissolved in the oil dispersion nor was it instantly saturated in the oil dispersion.

The CFD simulation approach was used to predict and assess the two-phase flow developments in different applications [13- 16]. [17] investigate the hydrodynamic characteristics of slug flow in a vertical pipe using the volume-of-fluid (VOF) methodology. This study provides a better understanding of the rise of an individual Taylor bubble through a stagnant liquid in pipes through performing dimensionless analysis treatment and employing Computational Fluid Dynamics (CFD) study that supports this developed logical approach to the problem. [9] used the CFD approach to simulate air-water two-phase flow in a pipe and to define some parameters such as pressure drop, void fraction and flow regime. The simulation results aligned with experimental results within a mean error of 20%. The CFD approach was also used to consider the bubbly flow in a vertical pipe using a Eulerian-Eulerian CFD two-phase model and to estimate the bubble size, bubble velocity and void fraction [18].

Some studies considered the two-phase flow patterns in different orientations. [10] reported an approach to predict flow patterns along upward inclined pipes (0–90°) via deep learning neural networks, using accessible parameters as inputs, namely, superficial velocities of individual phase and inclination angles. The predictive model was validated by comparing its outcomes with flow regime forecasting methods based on a flow pattern map. [19] numerically studied a Taylor flow in inclined pipe (0–90°) using the VOF methodology based on dimensionless treatment. One of the main results of this study is that in order to reduce and save the computational resources, a simplified model is suggested to solve the challenging problem of the three-dimensional Taylor bubble in near horizontal and horizontal pipes. [20] investigated the air-water two-phase flow in developing region. The operating condition in the test section was as follows: superficial air velocity: 0.02–0.87 m/s (at atmospheric pressure) and superficial water velocity: 0.01–0.2 0.01–0.2 m/s, which covers the range of bubbly to slug flow in a small-scale pipe (Dh $\leqslant$ about 0.05 m). The authors reported that void fraction near the top of the test section with Kataoka's correlation indicated that the distribution parameter of the drift-flux model should be modeled including the effect of hydraulic diameter and the bubble size distribution would be affected by the air injection methods.

Wire Mesh Sensors (WMSs) was used to predict the two-phase flow pattern which is based on the analysis of the time history of an area-averaged void fraction [2], [21- 26]. The WMS has the benefit of low coast and can get the phase arrangement behavior in the measurement’s plane with high resolution [25], [27- 29].

[22] reported on the flow regimes of a mixture containing nitrogen gas-water flowing in a vertical pipe using a Differential Pressure Transducer (DPT). The author stated that pressure fluctuations in the pipe were very nearly connected with the behavior of flow patterns. The outcomes showed the possibility of exploiting such devices for classifying the two-phase flow patterns in a vertical pipe. [23] utilized the non-intrusive Electrical Resistance Tomography (ERT) for evaluating the void fractions of gas-liquid flow in a horizontal pipe, contrasting the results with the DPT. The study reported that the DPT sensors gave reasonable agreement compared with ERT. The study also reported that the influence of the wall friction loss could be extracted when the mean void fraction of the gas phase was less than 0.2.

[24] investigated the flow regime of air-silicone oil flow in a riser vertical pipe. The author used Electrical Capacitance Tomography (ECT), Wire-Mesh Sensors (WMSs), and Differential Pressure Transducer (DPT) to estimate void fractions and flow patterns. Cap bubble, slug, and churn flows were observed in the experiments. The validation of using DPT was investigated by [4] in a pipe of an internal diameter of 50 mm with different orientations: 0, 30, 45 degrees. They ascertained that the pressure in the tested pipe dropped with the increase in void fractions and orientation degree respectively.

Despite the large number of studies investigating two-phase flow using different techniques and different working fluids, there is very limited information about air-water two-phase flow development considering the pressure drop along the vertical pipe. Thus, this study provides experiments and CFD simulations of air-water two-phase flow aiming to investigate the flow development in a vertical pipe and predict the pressure drop. Also, this study provides a real database for future experimental and computational research related to two-phase flow patterns, pressure drop, and void fractions investigations.

2. Experimental setup

The two-phase flow facility was designed and fabricated to operate an air-water two-phase flow in a vertical pipe. Figure 1 shows the schematic diagram of the facility.

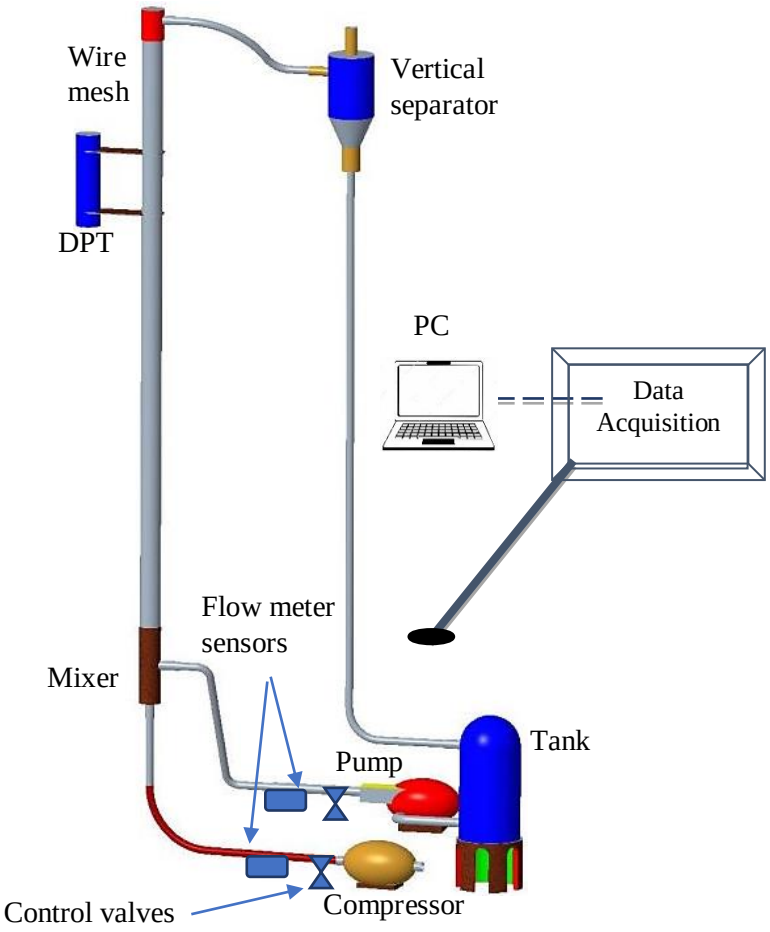

Fig.1. Schematic diagram for the two-phase facility.

A vertical pipe of 67 mm diameter and 7000 mm length was connected with a mixer to receive air and water after being very well mixed at the inlet of the pipe. Then, in a simple vertical separator, air and water were separated to be returned to a water tank for circulation. A water pump and air compressor were used to provide air and water to cover the range of operating conditions. Data acquisition was used to receive and record all the measured parameters such as pressure, temperature and mass flow rate. Differential Pressure Transducers (DPTs) and Wire Mesh Sensors (WMSs) were used to record and monitor the flow behavior and its developments. A wide range of the operating conditions was applied in the experiments of this study. While conducting experiments, the air superficial velocity range changed from 0.06 to 6 m/s, and the water superficial velocity was fixed at 0.2 and 0.5 m/s for all cases.

3. CFD Simulation and Setup

3.1 Multiphase flow model

Air and water were used as working fluids in CFD simulations to predict the two-phase flow developments in a vertical pipe. CFD software Fluent 16.2 was used to predict and assess the two-phase flow. The CFD approach is flexible and easy to use in different applications due to its efficient performance [4], [15], [30-33]. Volume of Fluid (VOF) two-phase model was selected to predict the two-phase flow behavior in the vertical pipe.

3.2 Geometry and mesh

Dimensions of the experimental test section which has a 67 mm diameter, and a length of 7000 mm were used to generate a three-dimensional geometry using a Design Modular of ANSYS 2021 R2. Air and water are mixed in the mixing section which play a crucial role to provide very well mix region at the inlet of the vertical pipe. Fig. 2. shows the mixing section of the meshed geometry. To confirm the independence of mesh, different mesh size was applied between 180000 and 1500000. By applying the assumption of the gas-liquid interface which defines the value of gas holdup was between 1 and zero, gas holdup was predicted and used to specify the ideal mesh size. In addition, the experimental value of pressure drop was also compared with the predicted vale to select the ideal mesh size. After a series of simulations, 850000 unstructured tetrahedral mesh was selected, which involved less computational time.

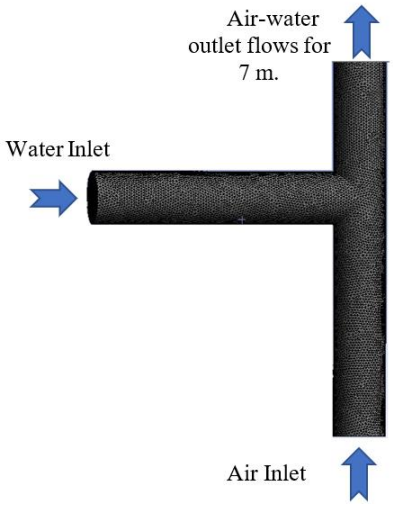

Fig. 2. 3D mesh geometry of the mixing section.

3.3 Boundary condition

The boundary conditions were applied to simulate the air-water two-phase flow in CFD. The velocity inlet was applied at the inlet and stationary wall with no slip was applied for the walls. The outlet boundary condition was atmospheric pressure outlet for all cases because the gas output of the vertical separator was open to the atmosphere. Smooth surface assumption was applied in simulations with consideration of the gravity effect. The surface tension between air and water was considered and applied. The experimental inlet superficial velocities for the air and water were used in all simulation cases.

3.4 Governing equations

In the present model, the method of the volume-of-fluid (VOF) for two-phase flow is selected which is a model based on the surface-tracking technique that can be adopted on a fixed Eulerian mesh that is due to, the fluids share a well-defined interface. This model is designed for two or more immiscible fluids to track the interface between them. A single set of momentum equations can be solved using this model. This set of equations are shared by the two fluids, and the volume fraction of each of the fluids in each computational cell is followed throughout the domain. Details of the governing equations and the treatment of the interface can be obtained from [34]:

One set of continuity and momentum equations are solved for the two-phase system. Firstly, the continuity equation in a VOF model for N number of phases can be expressed as follows.

$$\frac{\partial \rho}{\partial t} + \nabla . (\rho V) = \sum_{q=1}^{N} S_q \qquad (1)$$

For the present two-phase flow, N=2 and the mass source, S_q, is set to zero. For incompressible flow, Eq. (1) would result in the following form:

$$\nabla . V = 0 \quad (2)$$

In addition, the momentum equation is solved throughout the computational domain, and all phases share the same resulting velocity field. The momentum equation for unsteady incompressible flow can be written as follows:

$$\rho \left[\frac{\partial V}{\partial t} + (V.\nabla)V\right] = -\nabla P + \mu(\nabla.\nabla)V + F \quad (3)$$

The additional forces could be a gravitational term or surface tension. Thus, the lift hand side of Eq. (3) represents the unsteady term and convection terms. While the right-hand side represents the pressure term, the diffusion term, the body force, and other external forces that might act on the system. The surface tension at the gas-liquid interface is calculated using the continuum surface force (CSF) of [35], which is given by:

$$F_S = \sigma K n \quad (4)$$

The unit normal of the interface (n) is defined in terms of the volume fraction (α_G) as follows:

$$n = \nabla \alpha_G \quad (5)$$

and K is given by:

$$K = \nabla . \frac{\nabla \alpha_G}{|\nabla \alpha_G|} \quad (6)$$

The VOF formulation depends on the impossible interpenetration among two or more phases. There is new variable introduced in every added phase to the model, that is the volume fraction of the phase in the computational cell. For every single control volume, the volume fractions of all phases are one in total. If the volume fraction of the q^{th} fluid in a cell is given by α_q, thus the following relationship is valid for each computational cell:

$$\sum_{q=1}^{N} \alpha_q = 1 \quad (7)$$

As long as the volume fraction for each phase at each location is known, all variable and property are shared between phases. Therefore, depending upon the volume fraction values, in any given cell, the variables and properties are either purely represent the phases individually, or represents the mixture of the phases, [36], [37]. Hence, there are three possible conditions which can be applied based on void fraction values. The first condition is when $\alpha_q = 0$, the cell is empty of the q^{th} fluid. The second condition is when $\alpha_q = 1$, the cell is occupied mainly by the q^{th} fluid. Finally, if $0 < \alpha_q < 1$, the cell contains the interface between the q^{th} fluid and the other fluid.

The continuity and momentum equations both are depending on the volume fraction of phase through the volume-fraction-averaged properties ρ and μ. Hence, depending on the local value of α_q as discussed

above, the volume-fraction-averaged density and viscosity are calculated as follows:

$$\rho = \sum_{q=1}^{N} \rho_q \, \alpha_q \quad (8)$$

$$\mu = \sum_{q=1}^{N} \mu_q \alpha_q \quad (9)$$

In order to track the interface between the two phases, the volume fraction of the q^{th} fluid (α_q) can be monitored through solving a separate continuity equation which is given by [36], as follows:

$$\frac{1}{\rho_q}\left[\frac{\partial}{\partial t}(\alpha_q \rho_q) + \nabla.(\alpha_q \rho_q V_q)\right] = S_q + \sum_{p=1}^{n_{step}} (\dot{m}_{pq} - \dot{m}_{qp}) \quad (10)$$

According to [36], the source term (S_q) is set to zero. While the volume fraction will be used to solve the volume fraction of the q^{th} fluid (α_q) which represent the secondary phase not the primary phase. The gas phase is computed according to the constraint given in Eq. **Error! Reference source not found.**. For unsteady incompressible flow, Eq. **Error! Reference source not found.** can be written as follows:

$$\frac{\partial \alpha_q}{\partial t} + \nabla.\alpha_q V_q = 0 \quad (11)$$

3.5 CFD solution and procedure

A VOF two-phase flow model was used to predict the flow behavior and estimate the pressure drop of air-water two-phase flow in a vertical pipe. The transient solver was activated with 0.001 time step. PISO scheme and second order for the momentum and turbulent scheme were performed in the CFD simulations. Convergence was obtained and considered at 10-8 after changing the under-relaxation values.

4. RESULTS

Experiments and CFD simulations were completed to predict the air-water two-phase flow behavior and pressure drop in the vertical pipe. The wire mesh sensor recorded the tomographic images for the flow at different range of gas and water superficial velocities. The experimental operating conditions were used in CFD simulations to obtain consistency.

4.1 Flow behavior

Wire mesh sensors (WMSs) recorded a tomographic image for the flow in the vertical pipe at a different range of air superficial velocity and water superficial velocity. The WMS was located at 6.5 m from the inlet to record the outcome of the flow behavior. Fig. 3. shows the tomographic images of the WMSs at a different range of gas superficial velocity from 0.05 to 5 m/s. The liquid superficial velocity was fixed at two constant values of 0.2 and 0.4 m/s. As can be seen, different flow patterns were obtained such as bubbly flow at Usg of 0.064 m/s, slug flow at Usg from 0.3 to 0.9 m/s, and then churn flow from 2.5 to 4 m/s at fixed liquid superficial velocity Usl of 0.2 m/s.

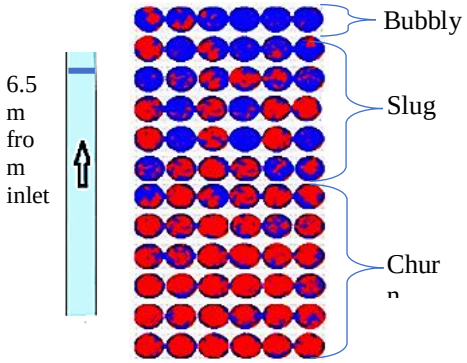

Fig. 3. Two-phase flow behavior at Usg range from 0.05 to 5 m/s and Usl 0.2 m/s, cross section plan in the developed regime (at 6.5 m from the inlet).

Fig. 4. shows the tomographic images at fixed liquid superficial velocity Usl of 0.4 m/s. As can be seen different flow patterns were obtained such as bubbly flow at Usg of 0.07 m/s, slug flow at Usg from 0.32 to 1.2 m/s and then churn flow from 1.5 to 5 m/s at fixed liquid superficial velocity Usl of 0.4 m/s.

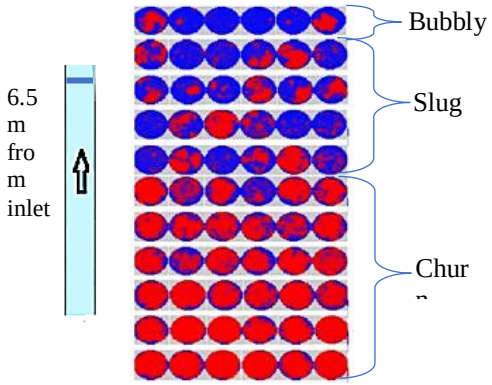

Fig. 4. Two-phase flow behavior at Usg range from 0.05 to 5 m/s and Usl 0.4 m/s, cross section plan in the developed regime (at 6.5 m from the inlet)

4.2 Pressure drops

Fig.5. and Fig. 6. show the comparison between the experimental results and CFD predictions of the pressure drop for the air-water two-phase flow at the range of the experimental operating conditions. The maximum experimental uncertainty of ± 23.5 was considered in the analysis of this work. From Fig. 5., the pressure drop is increased gradually from the minimum value of 16.5 Pa/m to the maximum valve of 568.7 Pa/m when the gas superficial velocity increased from 0.5 to 5 m/s and liquid superficial velocity of 0.2 m/s. The CFD results for the pressure drop were overestimated compared with the experimental result with maximum absolute error of 21%.

ISSN: 2096-3246
Volume 54, Issue 06, August, 2022

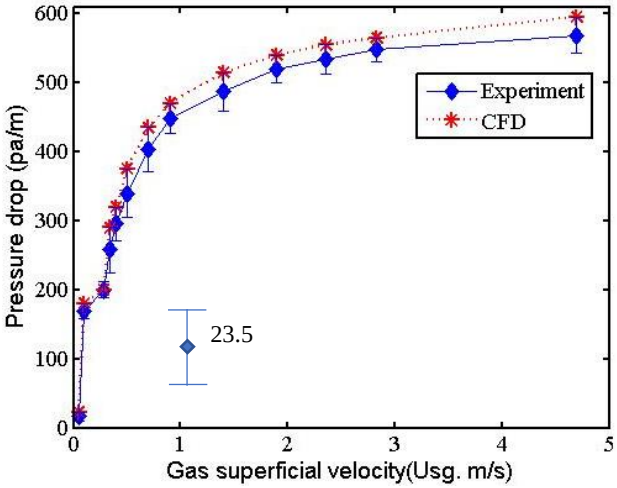

Fig.5. Comparison between experimental and CFD pressure drop at liquid superficial velocity of 0.2 m/s, maximum experimental uncertainty was ±23.5.

In Fig.6., the pressure drop increased gradually from the minimum value of 18.9 Pa/m to the maximum valve of 579 Pa/m when the gas superficial velocity increased from 0.5 to 5 m/s and liquid superficial velocity of 0.2 m/s. The CFD results for the pressure drop were over the experimental result with maximum absolute error of 25%.

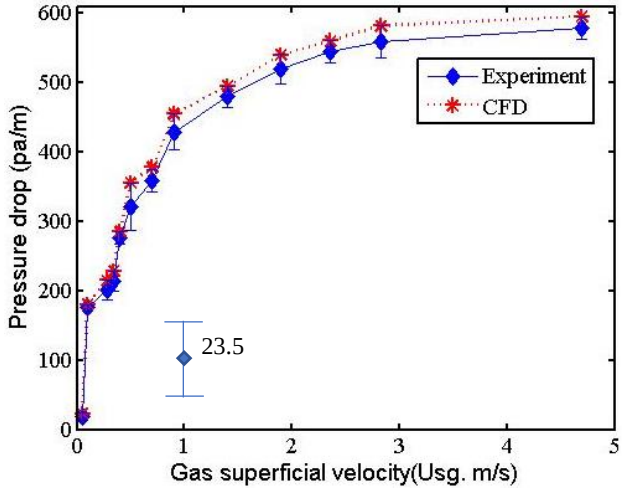

Fig.6. Comparison between experimental and CFD pressure drop at liquid superficial velocity of 0.4 m/s, maximum experimental uncertainty was ±23.5.

4.3 Two-phase flow pattern map

A two-phase flow pattern map was generated to present the observed behavior of the air-water two-phase flow patterns. The air-water two-phase flow pattern is presented in the map based on the change of liquid and gas superficial velocity. Fig.7. shows the outcome of this research including the CFD prediction for the air-water two-phase flow pattern. Bubbly, slug, plug and churn two-phase flow patterns were presented at liquid superficial velocity 0.2 m/s and 0.4 m/s with variation of gas superficial velocity from 0.05 m/s to 5 m/s.

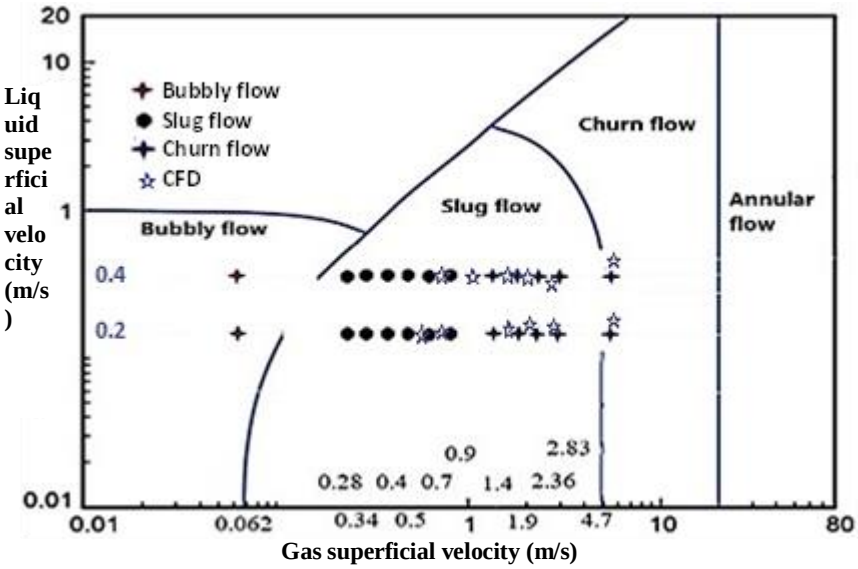

Fig.7. Two-phase flow pattern maps for the observed experimental and CFD behavior.

5. CONCLUSION

Air-water two-phase flow in a vertical pipe was studied in this research experimentally. The computational approach using ANSYS Fluent 2021 R2 was used to generate three-dimensional geometry. A VOF model was used to simulate and assess the air-water two-phase flow behavior in the vertical pipe. The outcomes of this research can be summarized as follow:

- There was no significant effect when the Usl changed from 0.2 m/s to 0.4 m/s on the vertical flow lines. The variation of Usg in the experiments, recorded a significant effect on the vertical flow.
- Bubbly flow was observed at Usg of 0.064 m/s when the Usl was 0.2 m/s. Then the flow changed to slug flow when the Usg range was between 0.3 and 0.9 m/s.
- Churn flow was observed at a range of Usg from 2.5 to 4 m/s at fixed liquid superficial velocity Usl of 0.2 m/s.
- When the Usl changed to 0.4 m/s, bubbly flow was observed at Usg of 0.07 m/s and slug flow was generated at the range of Usg from 0.32 to 1.2 m/s.
- At Usl of 0.4 m/s, churn flow was observed at the range of Usg from 1.5 to 5 m/s.
- The experimental pressure drop was presented with the change of gas superficial velocity and maximum uncertainty of ± 23.5 was recorded at Usl of 0.2 m/s. The pressure drop was increased gradually when the Usg increased. The CFD results of the pressure drop were overestimated compared with the experimental result when the Usl was equal to 0.2 m/s. The maximum absolute error of 21% was recorded.
- Pressure drop was recorded at Usl of 0.4 m/s and variation of gas superficial velocity range from 0.5 to 5 m/s with maximum uncertainty of ± 23.5. The pressure drop trend was increased gradually when the Usg increased. The CFD results of the pressure drop were overestimated compared with the experimental result when the Usl was equal to 0.4 m/s. The maximum absolute error of 25% was recorded.
- A two-phase flow pattern map was generated to present the experimental and CFD observations of the air-water two-phase flow patterns at the experimental operating conditions of the Usg range from 0.05 to 5 m/s and fixed velocity of Usl of 0.2 m/s and 0.4 m/s.

6. REFERENCES

[1] Mahmood, R., D. Buttsworth, and R. Malpress, Computational and Experimental Investigation of using an Extractor in the Vertical Gravitational Flash Tank Separator. International Journal of Automotive and Mechanical Engineering, 2019. 16(2): p. 6706-6722.

[2] Abdulkareem, L.A., et al., Experimental investigation of two-phase flow patterns in a vertical to horizontal bend pipe using wire-mesh sensor. Revista de Chimie, 2021. 71(12): p. 18-33.

[3] Santos, T.S.M.M., Hydrodynamics of gas-liquid flows in slug flow regime. 2007, Universidade do Porto (Portugal).

[4] Hameed, A.I., L.A. Abdulkareem, and R.A. Mahmood, Experimental Comparison Between Wire Mesh and Electrical Capacitance Tomography Sensors to Predict a Two-Phase Flow Behaviour and Patterns in Inclined Pipe. Technium, 2021. 3(5): p. 49-63.

[5] Musa, V.A., et al., Flow Patterns of Oil-Gas and Pressure Gradients in Near-Horizontal Flow Pipeline: Experimental Investigation Using Differential Pressure Transducers. Journal homepage: http://iieta. org/journals/ijht, 2021. 39(2): p. 621-628.

[6] Mahmood, R.A., et al., CFD Numerical and Experimental Investigation of Two-Phase Flow Development after Expansion Device in a Horizontal Pipe. Journal of Thermal Engineering, 2019.

[7] Lockhart, R., Proposed correlation of data for isothermal two-phase, two-component flow in pipes. Chem. Eng. Prog., 1949. 45(1): p. 39-48.

[8] Cao, Y., et al., Thermal characteristics of air-water two-phase flow in a vertical annularly corrugated tube. Journal of Energy Storage, 2020. 31: p. 101605.

[9] Kiran, R., R. Ahmed, and S. Salehi, Experiments and CFD modelling for two phase flow in a vertical annulus. Chemical Engineering Research and Design, 2020. 153: p. 201-211.

[10] Lin, Z., et al., Prediction of two-phase flow patterns in upward inclined pipes via deep learning. Energy, 2020. 210: p. 118541.

[11] Shadloo, M.S., et al., Estimation of pressure drop of two-phase flow in horizontal long pipes using artificial neural networks. Journal of Energy Resources Technology, 2020. 142(11): p. 112110.

[12] Yang, H., et al., The effect of interfacial mass transfer of slip-rising gas bubbles on two-phase flow in the vertical wellbore/pipeline. International Journal of Heat and Mass Transfer, 2020. 150: p. 119326.

[13] Mahmood, R.A., CFD Assessment and Experimental Investigation of the Liquid Separation Efficiency Enhancements in a Vertical Gravity Separator. International Journal of Air-Conditioning and Refrigeration, 2020. 28(03): p. 2050021.

[14] Mahmood, R.A., D. Buttsworth, and R. Malpress, Computational and experimental investigation of the vertical flash tank separator part 1: Effect of parameters on separation efficiency. International Journal of Air-Conditioning and Refrigeration, 2019. 27(01): p. 1950005.

[15] Mahmood, R.A., CFD Instruction Guide to Simulate Two-Phase Flow Separation in a Vertical T-junction Separator. International Journal of Advances in Science Engineering and Technology, 2019. 7(2).

[16] Mahmood, R.A., Experimental and computational investigation of gravity separation in a vertical flash tank separator in Faculty of Health, Engineering and Sciences - School of Mechanical and Electrical Engineering. 2018, University of Southern Queensland.

[17] Massoud, E., et al., Numerical study of an individual Taylor bubble rising through stagnant liquids under laminar flow regime. Ocean Engineering, 2018. 162: p. 117-137.

[18] Tas-Koehler, S., et al., CFD simulation of bubbly flow around an obstacle in a vertical pipe with a focus on breakup and coalescence modelling. International Journal of Multiphase Flow, 2021. 135: p. 103528.

[19] Massoud, E., Q. Xiao, and H. El-Gamal, Numerical study of an individual Taylor bubble drifting through stagnant liquid in an inclined pipe. Ocean Engineering, 2020. 195: p. 106648.

[20] Ohnuki, A. and H. Akimoto, An experimental study on developing air-water two-phase flow along a large vertical pipe: effect of air injection method. International journal of multiphase flow, 1996. 22(6): p. 1143-1154.

[21] Szalinski, L., et al., Comparative study of gas–oil and gas–water two-phase flow in a vertical pipe. Chemical engineering science, 2010. 65(12): p. 3836-3848.

[22] Ofuchi, C.Y., et al., Multiple wire-mesh sensors applied to the characterization of two-phase flow inside a cyclonic flow distribution system. Sensors, 2019. 19(1): p. 193.

[23] Prasser, H.-M., M. Misawa, and I. Tiseanu, Comparison between wire-mesh sensor and ultra-fast X-ray tomograph for an air–water flow in a vertical pipe. Flow Measurement and Instrumentation, 2005. 16(2-3): p. 73-83.

[24] Vieira, R.E., et al., Experimental characterization of vertical downward two-phase annular flows using Wire-Mesh Sensor. Chemical Engineering Science, 2015. 134: p. 324-339.

[25] Zhang, H., Y. Xiao, and H. Gu, Experimental investigation of two-phase flow evolution in a tight lattice bundle using wire-mesh sensor. International Journal of Heat and Mass Transfer, 2021. 171: p. 121079.

[26] Shaban, H. and S. Tavoularis, The wire-mesh sensor as a two-phase flow meter. Measurement Science and Technology, 2014. 26(1): p. 015306.

[27] Zhang, H., Y. Xiao, and H. Gu, A new method to determine conductivity distribution based on wire-mesh sensor by iteration. Annals of Nuclear Energy, 2020. 143: p. 107443.

[28] Prasser, H.-M., A. Böttger, and J. Zschau, A new electrode-mesh tomograph for gas–liquid flows. Flow measurement and instrumentation, 1998. 9(2): p. 111-119.

[29] Arai, T., et al., Development of a subchannel void sensor and two-phase flow measurement in 10× 10 rod bundle. International journal of multiphase flow, 2012. 47: p. 183-192.

[30] Mahmood, R., O.M. Ali, and M. Noor, Mechanical vapour compression refrigeration system: review part 1: environment challenge. International Journal of Applied Mechanics and Engineering, 2020. 25(4): p. 130-147.

[31] Mahmood, R.A., Case study of liquid suction heat exchanger in a mechanical refrigeration system using alternative refrigerants. International Journal of Engineering & Technology, 2020. 9(3): p. 644-649.

[32] Mahmood, R., et al., Review of mechanical vapour compression refrigeration system part 2: performance challenge. International Journal of Applied Mechanics and Engineering, 2021. 26(3): p. 119-130.

[33] Mahmood, R.A., Saleh, K., Musa, V.A., Massoud, E., Sharifian-Barforoush, A., Abdulkareem, L.A, Two-Phase Flow Development of R134a in a Horizontal Pipe: Computational Investigation. International Journal of Heat and Technology, 2021. 39(5): p. 1532-1540.

[34] FLUENT, A., 14.5, Theory Guide; ANSYS. Inc., Canonsburg, PA, 2012.

[35] Brackbill, J., D.B. Kothe, and C. Zemach, A continuum method for modeling surface tension. Journal of computational physics, 1992. 100(2): p. 335-354.

[36] Fluent, A., Theory Guide and User's Guide. Ansys Inc, USA, 2015.

[37] Ramzi, N.A.S., et al., FLOW INDUCED VIBRATION IN SQUARE CYLINDER OF VARIOUS ANGLES OF ATTACK. IIUM Engineering Journal, 2022. 23(1): p. 358-369.